Journal of the Physical Society of Japan
Vol. 77, No. 9, September, 2008, 093705

Observation of Exciton Polaritons in a ZnO Microcavity with HfO_2/SiO_2 Distributed Bragg Reflectors

Masaaki NAKAYAMA, Shingo KOMURA, Toshiki KAWASE, and DaeGwi KIM

Department of Applied Physics, Graduate School of Engineering, Osaka City University, Sugimoto, Sumiyoshi-ku, Osaka 558-8585

(Received June 5, 2008; accepted July 22, 2008; published September 10, 2008)

We have investigated the characteristics of the exciton polaritons in a ZnO microcavity. The microcavity consists of an effective one-wavelength thick ZnO active layer and HfO_2/SiO_2 distributed Bragg reflectors (DBRs) at the bottom and top. We adopted rf magnetron sputtering and pulsed laser deposition for the preparation of the DBR and ZnO layer, respectively. Angle-resolved reflectance and photoluminescence spectra demonstrate the formation of the cavity polaritons. The cavity polariton dispersions are analyzed using a phenomenological Hamiltonian for the coupling between the cavity photon and three kinds of fundamental excitons labeled A, B, and C. The vacuum Rabi splitting energy is estimated to be ~80 meV. The giant Rabi splitting energy reflects the large exciton oscillator strength of ZnO.

KEYWORDS: ZnO, microcavity, distributed Bragg reflector, exciton polariton, Rabi splitting, rf magnetron sputtering, pulsed laser deposition
DOI: 10.1143/JPSJ.77.093705

Semiconductor microcavities have attracted much attention from the aspect of controlling the optical responses of exciton polaritons in a strong exciton–photon coupling regime resulting in the formation of cavity polaritons.[1] The prominent applications of cavity polaritons are polariton lasing,[2,3] parametric polariton amplifiers,[4,5] Bose–Einstein condensation of polaritons,[6,7] and enhancement of entangled-photon generation,[8] which are attractive in semiconductor physics. Until now, GaAs-based microcavities have been major samples owing to the well-established method for the sample preparation using molecular beam epitaxy or metal–organic chemical vapor deposition (MOCVD). Recently, microcavities consisting of wide-gap semiconductors such as GaN[9–11] and ZnO[12,13] have been developed from the viewpoint of large exciton binding energies, 28 meV for GaN[14] and 61 meV for ZnO,[15] leading to the high stability of the excitonic system.

In this letter, we report on the fabrication of a ZnO-based microcavity with distributed Bragg reflectors (DBRs) and the observation of cavity polaritons. Note that the preparation method for the ZnO-based microcavity has not yet been established, which is mainly due to the problem of the fabrication of DBRs suitable for ZnO. In ref. 12, ZrO_2/MgO DBRs were prepared by pulsed laser deposition (PLD). On the other hand, in ref. 13, bottom and top DBRs were AlGaN/GaN and SiO_2/Si_3N_4 systems grown by MOCVD and remote plasma enhanced CVD, respectively. In the present work, we adopted rf magnetron sputtering for the preparation of HfO_2/SiO_2 DBRs at the bottom and top of the microcavity because the sputtering method is convenient and powerful for the deposition of oxide materials. For the ZnO active layer, we used PLD to grow a high quality film. The cavity polaritons were observed with angle-resolved reflectance spectroscopy and photoluminescence (PL) spectroscopy. The experimental results were analyzed by calculating the cavity polariton dispersions with a phenomenological Hamiltonian for the coupling between the cavity photon and excitons, where we consider the A, B, and C excitons peculiar to ZnO. In the earlier works on ZnO-based microcavities,[12,13] such a precise analysis was not discussed.

We prepared HfO_2/SiO_2 DBRs on a (0001) Al_2O_3 substrate and a ZnO active layer using rf magnetron sputtering. Commercially-supplied plates of HfO_2 with a purity of 3N and SiO_2 with a purity of 4N were used as the targets. The sputtering gas was Ar under a pressure of 1×10^{-2} Torr, and the substrate was not heated: almost at room temperature (RT). The growth rates of HfO_2 and SiO_2 were monitored using a crystal oscillator: 0.18 nm/s for HfO_2 and 0.10 nm/s for SiO_2. The ZnO active layer was deposited on the bottom DBR by PLD. The target was a commercially-supplied ZnO plate with a purity of 4N. The back pressure of the PLD chamber was $\sim 1 \times 10^{-8}$ Torr. The pressure of O_2 was 5×10^{-2} Torr, and the substrate temperature was 650 °C during the PLD process. The ablation laser was the fourth harmonic generation light (266 nm) of a pulsed YAG laser with a power density of $\sim 3\,J/cm^2$ and a repetition rate of 10 Hz. The average growth rate was ~0.02 nm/shot. We confirmed from X-ray diffraction patters (not shown here) that the ZnO layer is just oriented along the [0001] (c) axis. For optical properties, angle-resolved reflectance and PL spectra were measured at 10 K. The probe light of reflectance was a Xe lamp, and the reflected light was detected with a charge coupled device attached to a 32-cm single monochromator with a resolution of 0.2 nm. The excitation light of PL was a 325-nm line of a He–Cd laser with a power density of $\sim 10\,mW/cm^2$. The PL was detected with the same system used in the reflectance measurement. In addition, we characterized the spectral profiles of DBRs at RT using a double-beam spectrometer.

In the preparation of the ZnO-based microcavity, the thermal stability of the HfO_2/SiO_2 DBR is a key problem because the ZnO active layer was deposited at 650 °C on the bottom DBR prepared at RT. In order to examine the thermal stability, we annealed the HfO_2 (48 nm)/SiO_2 (65 nm) DBR with 9.5 periods at 650 °C for one hour in the PLD chamber under the deposition ambience condition. Figure 1 shows the transmittance spectra of the DBR

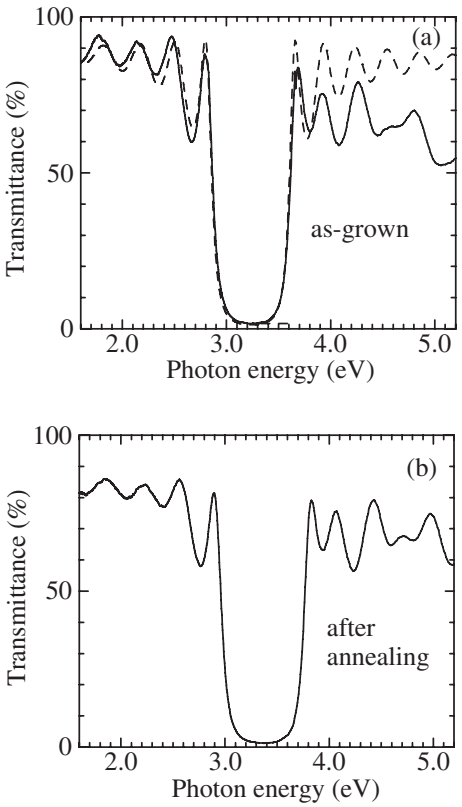

Fig. 1. Transmittance spectra of the HfO_2 (48 nm)/SiO_2 (65 nm) DBR with 9.5 periods in vertical incidence at RT (a) before (as-grown) and (b) after the annealing treatment. The dashed line indicates the calculated transmittance spectrum using a conventional transfer matrix method.

in vertical incidence at RT (a) before (as-grown) and (b) after the annealing treatment. The dashed line indicates the calculated transmittance spectrum using a conventional transfer matrix method, where the refractive indices of HfO_2 and SiO_2 are cited from ref. 16. The experimental spectrum is consistent with the calculated one, which suggests good controllability of the deposition process. The reduction in the transmittance in the energy region higher than that of the stop band is due to the absorption tail of HfO_2. It is evident from Fig. 1 that the spectral profile is robust to the annealing treatment, although the spectrum slightly shifts toward the high energy side. The energy region of the stop band covers the energies of the A, B, and C excitons of ZnO that are 3.378, 3.383, and 3.422 eV at 1.6 K, respectively.[15] The results described above demonstrate that the thermal stability of the HfO_2/SiO_2 DBR is sufficient for preparing the ZnO-based microcavity.

Figure 2 shows the angle-resolved reflectance spectra at 10 K in the effective one-wavelength (λ) thick ZnO microcavity with bottom and top HfO_2/SiO_2 DBRs consisting of 9.5 periods. The thickness of the ZnO layer is 190 nm. According to ref. 17 that deals with a bulk microcavity, we designed the effective cavity length, taking account of the background dielectric constant: $\varepsilon(\infty) = 3.70$ for ZnO.[15] The quality factor of the microcavity was estimated to be ~500 from an empty cavity. Four dip structures marked by closed and open circles appear in the energy region of the stop band of the DBR. Figure 3 shows the angle-resolved PL and reflectance spectra at the incident angles of 10, 20, and 30°. The energies of the PL bands that locate in the energy region higher than 3.25 eV do not change with the incident angle. Therefore, they are attributed to various bound excitons of ZnO. Note that the intensities of the bound exciton PL bands are affected by the angle dependent reflectivity of the DBR. On the other hand, the lowest energy PL band in each spectrum clearly depends on the incident angle, and its energy just agrees with that of the major reflectance dip. This fact indicates that the major reflectance dip is attributed to the lower polariton branch (LPB).

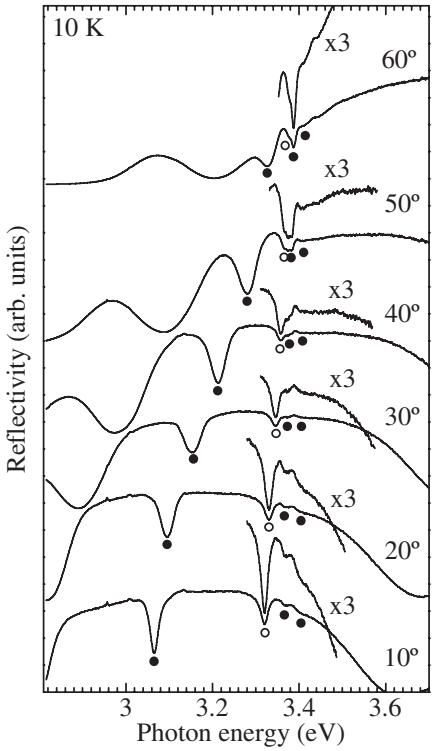

Fig. 2. Angle-resolved reflectance spectra at 10 K in the effective λ-thick ZnO microcavity with the HfO_2/SiO_2 DBRs at the bottom and top.

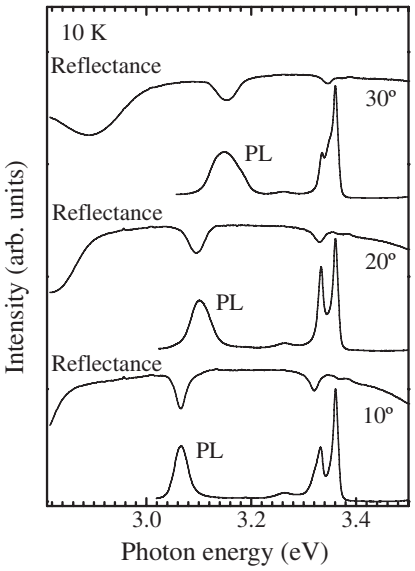

Fig. 3. Angle-resolved PL and reflectance spectra of the ZnO microcavity at the incident angles of 10, 20, and 30°.

We analyze the incident angle dependence of the energies of the four reflectance dips on the basis of a phenomenological Hamiltonian[1)] for the coupling between the cavity photon and three kinds of excitons labeled A, B, and C peculiar to ZnO. It should be noted that only the A exciton was taken into account in refs. 12 and 13. The Hamiltonian of the cavity polaritons is given by the following 4×4 matrix:

$$\begin{pmatrix} E_{\mathrm{ph}}(\theta) & \Omega_{\mathrm{A}}/2 & \Omega_{\mathrm{B}}/2 & \Omega_{\mathrm{C}}/2 \\ \Omega_{\mathrm{A}}/2 & E_{\mathrm{A}} & 0 & 0 \\ \Omega_{\mathrm{B}}/2 & 0 & E_{\mathrm{B}} & 0 \\ \Omega_{\mathrm{C}}/2 & 0 & 0 & E_{\mathrm{C}} \end{pmatrix}, \quad (1)$$

where E_{A}, E_{B}, and E_{C} are the energies of the A, B, and C excitons, respectively, and Ω_j is the vacuum Rabi splitting energy of the relevant exciton. Strictly speaking, the vacuum Rabi splitting, which has been conventionally used in semiconductor microcavities, should be regarded as normal mode splitting.[18)] $E_{\mathrm{ph}}(\theta)$ is the incident-angle (θ) dependent energy of the λ-cavity photon represented by[1)]

$$E_{\mathrm{ph}}(\theta) = \frac{hc}{n_{\mathrm{eff}} L_{\mathrm{c}}} \left(1 - \frac{\sin^2\theta}{{n_{\mathrm{eff}}}^2}\right)^{-1/2}, \quad (2)$$

where n_{eff} is the effective refractive index, and L_{c} is the cavity thickness. In this analysis, we do not consider the incident angle dependence of the Rabi splitting energies. It is known that the polarizations of the A and B excitons are perpendicular to the c-axis, while that of the C exciton is parallel to the c-axis;[19)] namely, the polarizations are anisotropic peculiar to the wurtzite structure. In ref. 9, the energies of four cavity polaritons observed in a wurtzite GaN microcavity are successfully analyzed using a phenomenological 4×4 Hamiltonian, in which the incident angle dependences of the Rabi splitting energies of Ω_{A}, Ω_{B}, and Ω_{C} are neglected. This indicates that the oscillator strengths of the excitons, which dominate the Rabi splitting energies, are independent of incident angle. Note that the spectral shape and intensity depend on the angle and polarization of incident light. Therefore, eq. (1) is valid for the analysis of the energies of the cavity polaritons in this case.

Figure 4 shows the incident angle dependence of the reflectance dip energies (closed and open circles) and fitted results (solid lines) of the cavity polaritons on the basis of eq. (1), where the closed and open circles correspond to the marks attached to the reflectance spectra shown in Fig. 2. In addition, the cavity photon dispersion and bare exciton energies are depicted by the dashed lines for reference. The cavity polaritons consist of four branches: the LPB, first middle polariton branch (MPB1), second MPB (MPB2), and upper polariton branch (UPB) as shown by the solid lines. The reflectance dip energies indicated by the closed circles are evidently assigned to the LPB, MPB1, and MPB2. The UPB could not be observed. Since the UPB locates in the energy region of the continuum states of the A and B excitons, mixing effects of the UPB and continuum states may weaken the oscillator strength of the UPB mode and broaden the line shape. This seems to be a probable reason for not observing the UPB. The values of the fitting parameters, n_{eff}, L_{c}, Ω_{A}, Ω_{B}, and Ω_{C}, are 1.92, 209 nm, 80, 140, and 80 meV, respectively. The value of n_{eff} is just consistent with the square root of the background

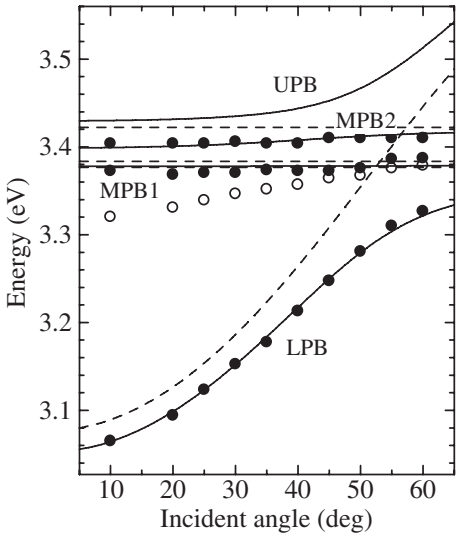

Fig. 4. Incident angle dependence of the reflectance dip energies (closed and open circles) and the fitted results (solid lines) of the cavity polaritons determined on the basis of eq. (1), where the closed and open circles correspond to the marks in Fig. 2. The dashed lines indicate the cavity photon dispersion and bare exciton energies.

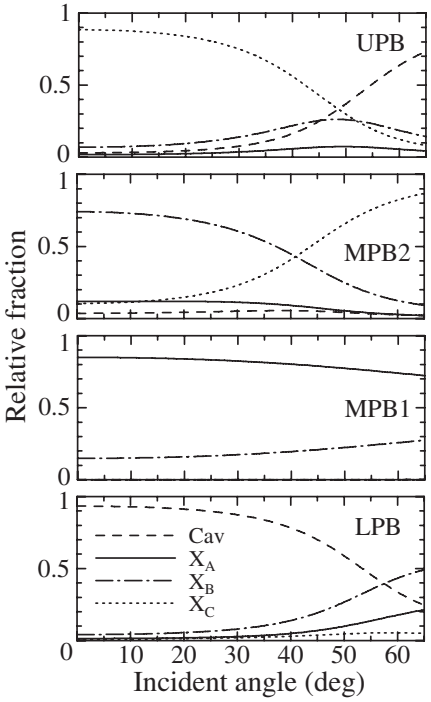

Fig. 5. Relative fractions of the cavity photon (Cav), A exciton (X_A), B exciton (X_B), and C exciton (X_C) in the cavity polaritons: They correspond to the squared eigenvectors calculated using eq. (1).

dielectric constant of ZnO. For L_{c}, the difference between the designed and fitted values is about 10%. Figure 5 shows the relative fractions of the cavity photon, A, B, and C excitons in the cavity polaritons: They correspond to the squared eigenvectors calculated using eq. (1). It is evident from Fig. 5 that the contribution of the C exciton is negligible for the LPB and MPB1, while that is dominant for the MPB2 and UPB. In this case, the UPB is not observed; therefore, Ω_{B} and Ω_{C} closely related to the MPB2 and UPB have ambiguity. On the other hand, Ω_{A} connected

with LPB and MPB1 is convincing. Namely, the Rabi splitting energy in the ZnO microcavity is estimated to be around 80 meV. In GaN-based microcavities, the reported Rabi splitting energies are ~25,[9] ~31,[10] and ~43 meV.[11] It is well known that the splitting energy between longitudinal and transverse excitons (Δ_{LT}) is a measure of the exciton oscillator strength: $\Delta_{LT} = 1.0$ meV for the A exciton of GaN[20] and 2.0 meV for that of ZnO.[15] Therefore, the giant Rabi splitting energy of ~80 meV reflects the large exciton oscillator strength of ZnO. In the earlier works on ZnO microcavities,[12,13] the Rabi splitting energy was estimated to be ~50 meV. The origin of the large discrepancy of the Rabi splitting energies is not clear. In bulk microcavities, the confinement of the photon field in the active layer markedly affects the Rabi splitting energy.[21] Thus, the discrepancy of the Rabi splitting energies may be due to differences of the DBR structures controlling the photon-field confinement.

In Fig. 4, it is obvious that the experimental results indicated by the open circle cannot be assigned to the cavity polaritons. In the reflectance spectra shown in Fig. 2, the unassigned signal marked by the open circle is the second major dip. From Fig. 4, it is evident that there is no anticrossing behavior between the unassigned mode and the cavity polaritons. This fact indicates that the unassigned mode does not interact with the cavity polaritons. Therefore, it is valid to neglect the effect of the unassigned mode in the analysis using eq. (1). The angle dependence of the unassigned mode looks like an LPB if we neglect the real LPB. Although we cannot reasonably explain the appearance of the unassigned mode, fluctuations of ZnO and/or DBR thicknesses may possibly produce another LPB-like mode.

In summary, we have fabricated the λ-thick ZnO microcavity with HfO_2/SiO_2 DBRs using rf magnetron sputtering for the DBR and PLD for the ZnO active layer. The cavity polaritons, LPB, MPB1, and MPB2, are observed from the angle-resolved reflectance spectra. The LPB is also detected by the angle-resolved PL spectra. The dispersions of the cavity polaritons have analyzed with the phenomenological 4×4 Hamiltonian for the coupling between the cavity photon and excitons labeled A, B, and C. The Rabi splitting energy is estimated to be around 80 meV, which reflects the large exciton oscillator strength of ZnO.

Acknowledgment

This work was supported by a Grant-in-Aid for Creative Scientific Research (No. 17GS1204) from the Japan Society for the Promotion of Science.

1) For a review, M. S. Skolnick, T. A. Fisher, and D. M. Whittaker: Semicond. Sci. Technol. **13** (1998) 645.
2) A. Imamoglu, R. J. Ram, S. Pau, and Y. Yamamoto: Phys. Rev. A **53** (1996) 4250.
3) G. Malpuech, A. Kavokin, A. Di Carlo, and J. J. Baumberg: Phys. Rev. B **65** (2002) 153310.
4) P. G. Savvidis, J. J. Baumberg, R. M. Stevenson, M. S. Skolnick, D. M. Whittaker, and J. S. Roberts: Phys. Rev. Lett. **84** (2000) 1547.
5) M. Saba, C. Ciuti, J. Bloch, V. Thierry-Mieg, R. André, Le Si Dang, S. Kundermann, A. Mura, G. Bongiovanni, J. L. Staehli, and B. Deveaud: Nature **414** (2001) 731.
6) M. Richard, J. Kasprzak, R. André, R. Romestain, Le Si Dang, G. Malpuech, and A. Kavokin: Phys. Rev. B **72** (2005) 201301.
7) R. Balili, V. Hartwell, D. Snoke, L. Pfeiffer, and K. West: Science **316** (2007) 1007.
8) H. Ajiki and H. Ishihara: J. Phys. Soc. Jpn. **76** (2007) 053401.
9) R. Butté, G. Christmann, E. Feltin, J.-F. Carlin, M. Mosca, M. Ilegems, and N. Grandjean: Phys. Rev. B **73** (2006) 033315.
10) I. R. Sellers, F. Semond, M. Leroux, J. Massies, M. Zamfirescu, F. Stokker-Cheregi, M. Gurioli, A. Vinattieri, M. Colocci, A. Tahraoui, and A. A. Khalifa: Phys. Rev. B **74** (2006) 193308.
11) A. Alyamani, D. Sanvitto, A. A. Khalifa, M. S. Skolnick, T. Wang, F. Ranalli, P. J. Parbrook, A. Tahraoui, and R. Airey: J. Appl. Phys. **101** (2007) 093110.
12) R. Schmidt-Grund, B. Rheinländer, C. Czekalla, G. Benndorf, H. Hochmut, A. Rahm, M. Lorenz, and G. Grundmann: Superlattices Microstruct. **41** (2007) 360.
13) R. Shimada, J. Xie, V. Avrutin, Ü. Özgür, and H. Morkoç: Appl. Phys. Lett. **92** (2008) 011127.
14) I. Vurgaftman and J. R. Meyer: J. Appl. Phys. **94** (2003) 3675.
15) E. Mollwo: in *Physics of II–VI and I–VII Compounds, Semimagnetic Semiconductors*, ed. O. Madelung, M. Schulz, and H. Weiss (Springer, Berlin, 1982) Landolt-Börnstein New Series, Group III, Vol. 17, p. 35.
16) A. J. Waldorf, J. A. Dobrowolski, B. T. Sullivan, and L. M. Plante: Appl. Opt. **32** (1993) 5583.
17) Y. Chen, A. Tredicucci, and F. Bassani: Phys. Rev. B **52** (1995) 1800.
18) S. Jorda: Phys. Rev. B **50** (1994) 18690.
19) D. G. Thomas: J. Phys. Chem. Solids **15** (1960) 86.
20) A. V. Rodina, M. Dietrich, A. Göldner, L. Eckey, A. Hoffmann, Al. L. Efros, M. Rosen, and B. K. Meyer: Phys. Rev. B **64** (2001) 115204.
21) A. Tredicucci, Y. Chen, V. Pellegrini, M. Börger, L. Sorba, F. Beltram, and F. Bassani: Phys. Rev. Lett. **75** (1995) 3906.